STUDY OF THE STRESS STATE FOR GEARS USED IN TRANSMISSIONS FOR POWER PLANTS

Mihai BUCUR*[1], Sorin CANANAU[2], Radu MIRICA[3], Cosmina CHIUJDEA [4]

This article presents a direct experimental methodology for mapping the stress distribution at the tooth root of helical gears. The work focuses on two fundamental aspects: (1) evaluating and determining the stress distribution at the tooth base through advanced experimental methods, such as strain gauge measurements and photoelastic analysis, under various loading and operating conditions; and (2) investigating the influence of specific factors in helical gears, such as misalignments and geometric modifications, on the stress profile at the root fillet. The experimental system was created and tested within in-depth studies conducted by the authors, to provide a solid database for validating numerical simulations and improving design processes.

Keywords: helical gears; root stress; stress distribution.

1. Introduction

The critical role of mechanical transmissions in the energy sector imposes stringent requirements for reliability and efficiency. Gear failure in wind turbine speed increasers or other rotating equipment represents a major cause of unplanned shutdowns. Such failures are almost always initiated by fatigue cracks at the tooth root, where stress concentrations occur. Although analytical and simulation models exist to estimate these stresses, experimental data are essential for validating these models and capturing effects that are difficult to simulate. This article presents a direct experimental methodology for mapping these critical stresses.

While numerical methods such as Finite Element Analysis (FEA) are powerful tools in modern gear design, they often rely on idealized conditions. Therefore, experimental analysis plays an indispensable role in validating and refining computational simulations. Experimental measurements provide crucial confirmation of calculated results by taking into account real operating conditions, material imperfections, and complex interactions that theoretical models do not fully capture.

[1] Eng., Dept. of Naval department, INCDTM Comoti, e-mail: mihai.bucur@comoti.ro
* Corresponding author, mihai.bucur@comoti.ro
[2] Prof., National University of Science and Technology POLITEHNICA Bucharest, Romania
[3] Assoc. prof., National University of Science and Technology POLITEHNICA Bucharest, Romania
[4] PhD, National University of Science and Technology POLITEHNICA Bucharest, Romania

Recent studies also emphasize the complementarity between experimental and numerical approaches. For example, [1] demonstrated that finite element simulations of optimized gear systems significantly reduce stress concentrations, confirming the need for accurate experimental validation. Similarly, [2] showed that geometric optimization of spur gears, such as introducing local design modifications at the tooth root, can lower bending stress by up to 25%. These findings support the necessity of combining experimental methods with advanced design strategies to enhance gear reliability.
In this context, strain gauge transducers remain a fundamental technology for localized and accurate strain measurement. [3]

2. Specific configurations for spur and helical gears

Strain gauges are successfully applied for measuring tooth root stresses in both spur gears and helical gears under static conditions.[4]

- spur gears: for spur gears, gauges are often cemented at the tooth root to estimate strain and stress. [4] calibration is performed by applying a controlled load to a single tooth, after adjacent teeth have been removed to isolate the tested tooth, ensuring precise measurement of the load response under static conditions.
- helical gears: in the case of helical gears, which transmit loads uniformly across the entire tooth width due to their tooth inclination [5], static measurements with strain gauges are equally relevant. a notable example is the measurement of tooth root stresses in large pinions, such as those used in marine applications. here, strain gauges are attached in the tooth fillet region of the pinion, and wires are routed through its interior to a signal acquisition system.[6] this method allows for the evaluation of load distribution along the tooth width, a crucial aspect for wide-faced gears.[4]

3. Specific Applications in static regime

Strain gauges are used in static conditions for:

- applied torque measurement: through a torque measuring shaft equipped with calibrated sensors.[7]
- load distribution evaluation: in planetary gears, to determine the load distribution factor on planet teeth, by measurements at the sun gear tooth root.
- numerical model validation: static measurements with strain gauges are used to validate analytical and numerical models (such as finite element method - fem) by direct comparison of experimentally obtained stress distributions with calculated ones.

- crack initiation detection: strain gauges can act as indicators of crack growth at the tooth root, in combination with visual observations, even in static fatigue tests where a crack is initiated at the tooth root.[8]

4. Advantages and considerations

Strain gauges are preferred in laboratory measurements due to their high sensitivity, precision, and small size.[9] They are resistant to vibration and shock and can operate at high temperatures and pressures, being placeable even on curved surfaces.[8] Thermally compensated strain gauges are available, designed to minimize errors induced by temperature variations.[10] For long-term static applications, alloys like K-alloy are recommended for their excellent stability.[11]
A recent generation of optical strain gauges offers an optimal solution for high-strain tests, where conventional electrical gauges can quickly reach their limits. [7] These can withstand 10 million stress cycles in continuous vibration behavior with alternating strain of ±5,000 μm/m and are suitable for measurements in potentially explosive atmospheres or on components subjected to high currents and voltages. [7] An additional advantage is the possibility of using multiple sensors in a single optical fiber, significantly reducing installation effort.[7]

5. Experimental methodology and test stand

The test stand is a laboratory device designed for the experimental determination of stress and strain states occurring in the tooth flanks of gears. It was developed specifically for the analysis of helical gears with large face widths, using the resistive strain gauge method to obtain quantitative data. Through its design, the equipment allows a realistic simulation of the behavior of a gear tooth throughout its entire operating cycle—from meshing entry to exit—providing a comprehensive picture of bending stresses. The stand is not an independent device but functions as an attachment to a universal mechanical testing machine for compression. The universal machine generates the testing force, while the stand is responsible for receiving and applying this force in a controlled manner, tangentially to the surface of the test tooth. In this way, the bending moment that underpins the analysis is generated. This setup is clearly illustrated in Figure 1, where the stand is shown in the initial loading position.
From a structural point of view, the stand consists of a robust base frame (1) on which a movable longitudinal slide (2) is mounted. The experimental gear wheel (used as a test specimen) (6) is fixed on this slide using two inclined supports: an upper support (7) and a lower support (12), which position the gear at an angle identical to the helix angle of the teeth. To prevent the gear from rotating during force application, an adjacent tooth to the one being tested rests against a fixed prism (15), as shown in Figure 2.

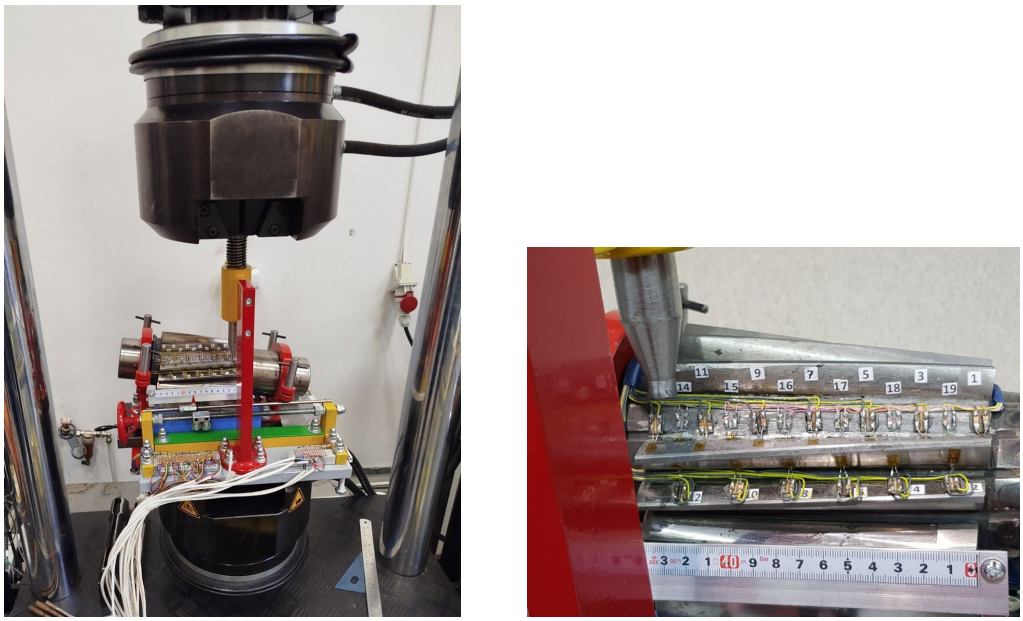

(a|) (b)

Fig. 1. Image of the test stand mounted on the compression testing machine
(a) test stand; (b) data acquisition instrumentation

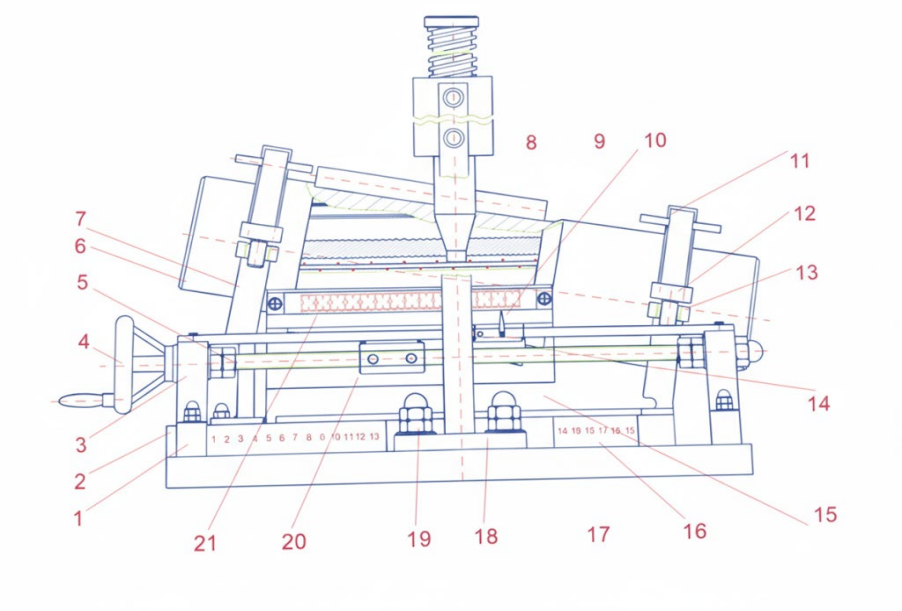

Fig. 2. Schematic of the test stand (front view)

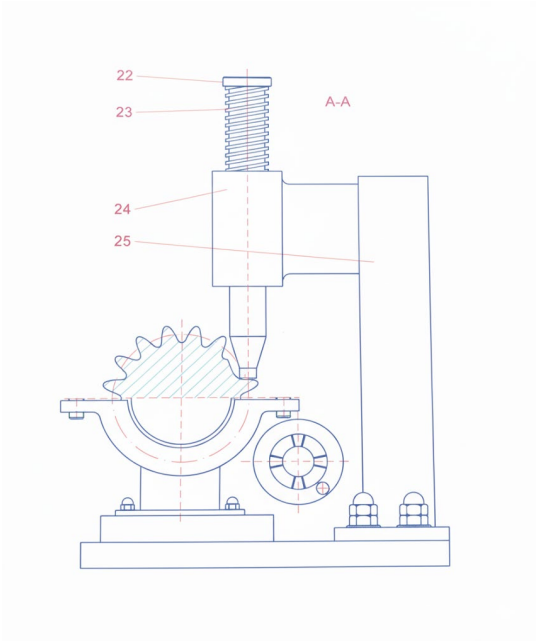

Fig. 3. Schematic of the test stand (side view)

The actual measurements are carried out using strain gauges (9), which are applied at equal intervals on the active flank of the test gear tooth (8). Similar gauges are also mounted on the passive flank, positioned in between those on the active side. The force is applied by a loading probe (22), which presses locally on the tooth in the spaces between the strain gauges on the active flank. Fine positioning of the probe along the tooth is achieved by moving the longitudinal slide (2) using a self-locking lead screw (5), operated manually via a handwheel (4). The linear displacement of the slide is precisely controlled with the aid of a graduated scale (21) and an indicator needle (10). A detailed visual, corresponding to Figure 6, is essential here to show the exact placement of the strain gauges (9) on the tooth flanks.

The experimental procedure is rigorous in order to ensure the accuracy of the data. For each measurement point, the probe (22) is carefully positioned, after which the compression machine applies a progressively increasing load, strictly within the elastic range of the material. Once the maximum load is reached, the compression machine's ram is lifted, and a return spring (23) automatically retracts the probe (22) to prevent damage to the strain gauges (9) during the slide's repositioning to the next measurement point.

The data from the strain gauges (9) are collected through a Wheatstone bridge and transmitted to a computer. Dedicated software processes this data and generates force-strain graphs for each load application point. These results allow for highly precise and detailed analysis of the stresses and strains along the entire tooth

length, making them extremely valuable for both the design and manufacturing processes of such gear systems. Thanks to its operating method, the test stand is user-friendly and well-suited for research engineers.

6. Validation and accuracy assurance of the experimental tests

To validate and ensure the accuracy of the experimental tests, six distinct test sets were performed. Each set followed the same standardized procedure:
The testing apparatus was initially positioned in Load Position 1, and the first force value was applied. This force was maintained constant for 10 seconds, during which the experimental data were recorded. The procedure was then repeated for each loading step until the maximum force value was reached.
Subsequently, the force was withdrawn, and the device was repositioned to Load Position 2, with the same steps repeated. This cycle continued until Load Position 6 was completed, thus marking the end of one full test set.
This repetitive methodology aimed to minimize positioning errors and potential fluctuations in electrical load—factors that are difficult to control even when using a voltage stabilizer.
The data acquisition process involved collecting 30 measurement values during each 10-second loading interval. These data sets were then processed by calculating the arithmetic mean, resulting in one average value per test. Initially, six average values were obtained, which were then subjected to an additional averaging step.
To ensure data reliability, a validation criterion was applied: each of the six initial average values was checked to ensure it deviated no more than 5% from the overall average. In cases where the deviation exceeded the set threshold, the value with the greatest discrepancy was removed, and the average was recalculated. This iterative procedure allowed for the exclusion of outlier values from the experimental data sets, thereby enhancing the precision of the results.
After these analyses, the following final set of values was obtained, with outliers eliminated:
In order to optimize the analysis process, a series of graphical representations were developed. Considering that seven strain gauges were placed on the active flank of the tooth, positioned laterally with respect to the pin axis, the average of their recorded values was calculated. This approach resulted in three distinct graphs, each containing six values corresponding to the six investigated pin positions. As shown in Figure 4, positions P1, P2, P5, and P6 correspond to a two-tooth engagement scenario, characteristic of the entry and exit phases of contact.

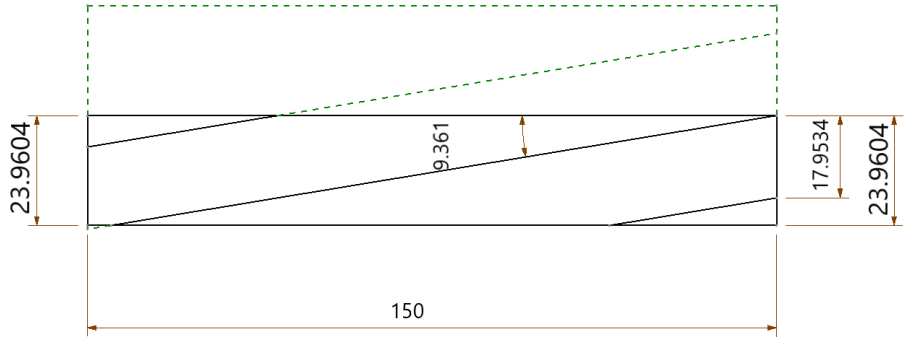

Fig. 4. Engagement lines

To more accurately approximate the stress distribution in a gear operating under real conditions—where the load is shared among multiple teeth—the values obtained using the pin were reduced to 60% of their initial level. This adjustment allows for a more realistic estimation of the actual stresses occurring during operation. Throughout this study, P1–P6 denote the measurement points positioned along the line of action, corresponding to successive contact locations during gear meshing

Table 1

Strain gauges on the active flank

	P1	P2	P3	P4	P5	P6
1	23,42979	12,30101	0,165487	0,057083	0,019628	0,006335
3	8,492843	19,83877	3,297888	0,559108	0,069508	0,02554
5	0,239615	8,769058	6,057017	3,37161	0,479462	0,104665
7	0,082173	0,490658	3,041478	5,734708	4,538842	0,536245
9	0,007888	0,054458	0,127137	3,020433	7,225905	3,313295
11	0,001063	0,01531	0,01737	0,222725	3,320217	6,529005

Table 2

Strain gauges on the passive flank

	P1	P2	P3	P4	P5	P6
1	85,01495	4,51047	0,27417	0,01391	0,002247	0,000957
3	2,271813	47,5474	1,213013	0,29043	0,01825	0,008687
5	0,180737	3,566023	10,25146	2,571567	0,337547	0,015493
7	0,03324	0,50836	1,669307	7,243123	2,5241	0,375577
9	0,00564	0,09392	0,354097	1,51833	13,21357	2,546077
11	0,0002	0,012037	0,04718	0,272363	1,680817	10,90116

Table 3

Fillet

	P1	P2	P3	P4	P5	P6
1	106,3605	22,8508	0,58148	0,025603	0,012	0,007923
3	13,21814	71,82006	7,633853	0,36656	0,00604	0,006567
5	0,18798	22,50467	6,44009	9,922437	0,39696	0,00586
7	0,05616	0,520787	11,54528	8,758757	11,35414	0,520277
9	0,00188	0,001643	0,29596	9,266757	31,99579	8,63207
11	0,002807	0,015833	0,03412	0,247893	10,88034	7,42286

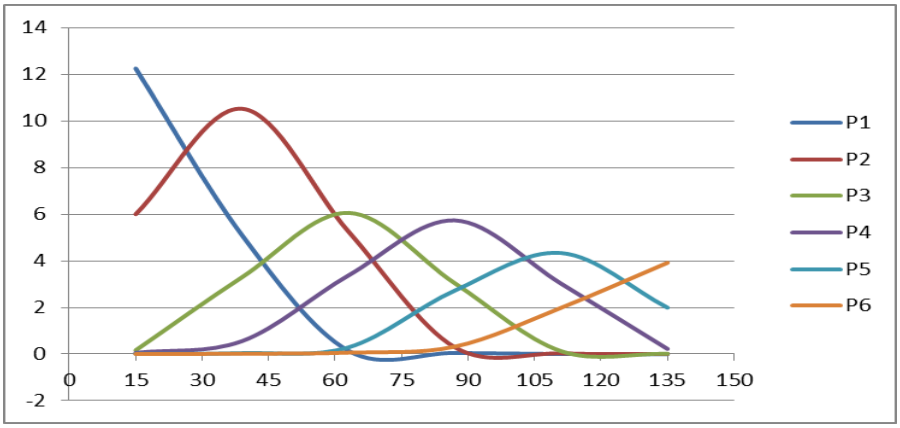

Fig.5 Active flank — 13 kN charge

As can be seen from Fig. 5, there is a distribution of the stress state that attests to the elastic behavior of the tooth, with a nonlinear effect, with high deformation and stress in the area of load application. As shown in the graphs, both on the active flank and the passive flank, the stress distribution is significant over a length of approximately 30 mm to the left and right of the roll position.

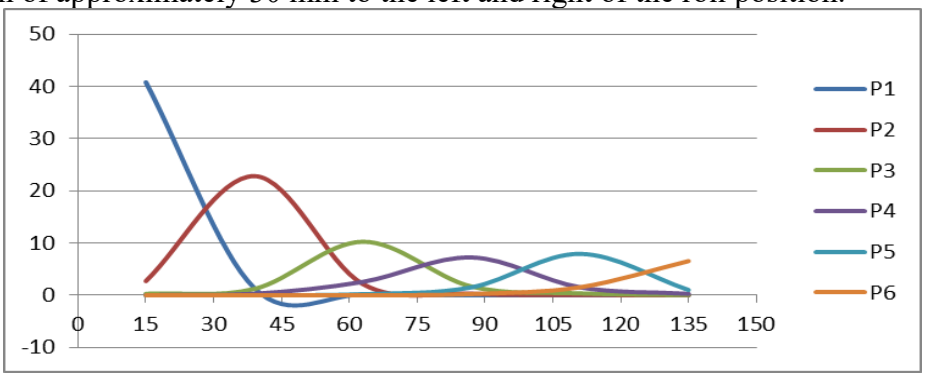

Fig.6 Passive flank — 13 kN charge

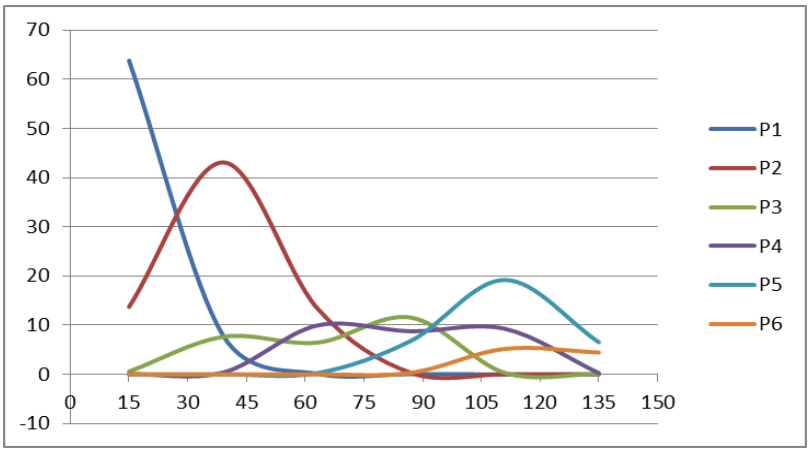

Fig.7 Fillet radius — 13 kN charge

Outside this zone, the values approach zero. Although some curves appear to dip slightly below zero, this phenomenon is caused by the steep slope of the variation as stresses decrease from values at least 20 times higher. In reality, all values remain positive.

On the active flank, the stress peak systematically shifts from position 1 (tooth tip) toward position 6 (tooth root), spanning about 30 mm in both directions relative to the center of the contact zone. This phenomenon reflects the sequential engagement and disengagement of the flank surfaces with the roll, followed by sliding and load transfer to lower zones. On the active flank, stresses are significantly lower than on the passive flank because two opposing types of loads act here:

• Bending of the tooth, which tends to stretch the strain gauge, and

• Crushing of the tooth, which tends to compress the gauge.

This dual loading attenuates the stress peaks compared to the passive flank, where a single compressive component dominates at the entry into contact.

In the fillet region of the tooth root, values exceed 63 MPa at position 1, much higher than those on the flanks. This highlights the importance of an appropriate fillet radius to avoid stress concentrations and fatigue cracks.

• Approximate symmetry in the contact zone length, but with different magnitudes

Although the length of the zone with significant stresses (≈30 mm) is similar on both flanks, the magnitude and shape of the stress curves differ. Under real operating conditions, this asymmetry explains the more pronounced pitting wear on the passive flank and the fatigue risk on the active flank.

7. Conclusions

- Successful Stress Mapping: The developed test stand and methodology proved highly effective in mapping the stress profiles along the active and passive flanks of the gear tooth. The system's ability to precisely control the point of load

application allowed for a detailed, point-by-point analysis of how stresses evolve during the meshing cycle.

- Confirmation of Critical Stress Location: The experimental data consistently showed that the maximum stresses occur in the fillet region of the tooth root. The measurement of values exceeding 63 MPa at this location underscores its vulnerability and confirms it as the primary site for fatigue crack initiation, validating a core principle of gear design.
- Asymmetric Flank Loading: A significant difference in stress magnitude was observed between the active and passive flanks. The analysis revealed that on the active flank, the combination of tensile stress from bending and compressive stress from local contact pressure results in attenuated stress peaks compared to the passive flank. This asymmetry is crucial for understanding distinct wear patterns, such as fatigue on the active flank and pitting on the passive flank.
- Validation of a Robust Procedure: The meticulous data acquisition protocol—involving multiple test sets, data averaging, and the systematic exclusion of outliers based on a 5% deviation criterion—ensured the reliability and accuracy of the final results. The adjustment of values for two-tooth contact scenarios represents a pragmatic approach to better approximate real-world load-sharing conditions.

REFERENCES

[1] *Sokolov, A*. (2025). Finite element analysis of stress distribution in optimized gear systems. Journal of Mechanical Engineering, 78(4), 345–359.
[2] *Hamzah, R., & Merza, F*. (2023). Geometric optimization of spur gears for stress reduction and enhanced performance. International Journal of Mechanical Design, 12(2), 112–128.
[3] FZG. (2009). Determination of load distribution in gears by means of strain gauges. Forschungsstelle für Zahnräder, Maschinenkonstruktion und Getriebebau.
[4] *Niemann, G., & Winter, H*. (1983). Machine Elements, Vol. 2: Transmissions in General, Gear Transmissions – Fundamentals, Spur Gear Transmissions. Springer-Verlag.
[5] *Retzel, H*. (2008). Measuring tooth root stresses on a large marine gear unit. Hottinger Baldwin Messtechnik (HBM) Report.
[6] HBM. (2012). Optical Strain Gauges. HBM.
[7] *Pedrero, J. I., Olmeda, P., & Antona, J. I.* (2007). Static test for determining the tooth root bending strength of spur and helical gears. Fatigue & Fracture of Engineering Materials & Structures, 30(3), 235-243.
[8] Hoffmann, K. (2005). An Introduction to Measurements using Strain Gages. Hottinger Baldwin Messtechnik (HBM).
[9] HBM. (n.d.). Properties of Strain Gauges. HBM.
[10] Micro-Measurements. (2010). Tech Note TN-505-1: Strain Gage Selection—Criteria, Procedures, Recommendations. Vishay Precision Group.